

SPECTROSCOPY OF NEON RYDBERG STATES DETECTED BY ELECTRON TRANSFER TO SF₆ MOLECULES

K. HARTH, M. RAAB, J. GANZ, A. SIEGEL, M.-W. RUF and H. HOTOP

Fachbereich Physik der Universität, 6750 Kaiserslautern, Fed. Rep. Germany

Received 29 March 1985

We have studied the ionization of laser excited $^{20}\text{Ne}(ns, md)$ Rydberg states in thermal energy collisions with SF₆ molecules as a means of sensitive detection of electronically excited states with binding energies from zero up to at least 0.4 eV. Effective collisional ionization was observed for $n \geq 8$, $m \geq 6$, but not for the Ne(5s)-, the Ne(4d)-, and other lower-lying Ne-states. A precise value for the ionization limit $^{20}\text{Ne}^+(^2\text{P}_{3/2})$ has been derived from Doppler free laser spectroscopy of the unperturbed $^{20}\text{Ne}(md, J=4)$ series ($m=4, 6-72$).

1. Introduction

Highly excited Rydberg states of atoms and molecules have been studied in detail during the past ten years using laser excitation techniques [1]. In most cases, state selective field ionization has been used for detection [2], but ionization of Rydberg states in collisions with (gas covered) surfaces [3] or with atoms [4] and molecules [5] in the gas phase can also be very effective. In 1967, Hotop and Niehaus [6] reported absolute cross sections for ionization of Rydberg states of He, Ne, and Ar atoms in thermal energy collisions with several polar molecules and with SF₆. Their experiments were carried out with a mixture of (n, l) states with n ranging from about 17 to 27, as can be inferred from their experimental conditions [7]. They found ionization cross sections in the range 10^{-13} – 10^{-12} cm² [6]. Later, more detailed experiments including work with selected (n, l) states [5] confirmed the early results and shed light on the ionization mechanism.

Target molecules M such as SF₆ are of particular interest: they are known to attach slow free electrons with large cross sections to form long-lived negative ions [8]



In collisions with Rydberg atoms A**, these molecules attach the weakly bound electron in the domi-

nating charge transfer process



The rate constants for processes (1) and (2) have been found [5] to be essentially the same for comparable electron velocities, and this result supports the quasi-free (or "essentially free" [5]) electron model [9] which views the A** + M collision as equivalent to an $e^- + M$ collision.

We have carried out a series of experiments, in which $^{20}\text{Ne}(ns, nd)$ Rydberg atoms, selectively prepared by two-step transverse laser excitation of a metastable Ne(3s $^3\text{P}_{2,0}$) beam, collided with a thin target of SF₆ molecules (densities below 10^{12} /cm³). $^{20}\text{Ne}^+$ ions, produced in collisions with SF₆, were detected with a quadrupole mass-spectrometer. We found effective ionization of Rydberg states with binding energies as high as 0.38 eV. We recommend the collisional ionization techniques as an attractive alternative detection method for states which cannot be easily field ionized and, therefore, are normally monitored by fluorescence. Using this collisional Rydberg detection scheme, we have determined the energy positions of a large number of Ne($ns, J=1, 2$) and Ne($nd, J=1, 2, 3, 4$) states by Doppler free laser spectroscopy. In this communication, we present the results for the unperturbed Ne($nd, J=4$) series ($6 \leq n \leq 72$), from which we deduce an improved value for the location of the Ne⁺(2p⁵ $^2\text{P}_{3/2}$) ionization limit relative to the position of the Ne(3s $^3\text{P}_2$) state.

2. Experimental method

The general experimental setup has been described elsewhere [10], here we emphasize the modifications relevant for the present work. The $^{20}\text{Ne}(3s\ ^3\text{P}_2)$ fraction of a well collimated (1 : 400), thermal velocity (800 m/s), metastable $\text{Ne}(3s\ ^3\text{P}_{2,0})$ beam (flux $2 \times 10^9/\text{s}$, density $3 \times 10^6/\text{cm}^3$), which emerges from a differentially pumped cold cathode discharge, was transversely excited to the $\text{Ne}(3p)$ intermediate state of interest by a stabilized single frequency cw dye laser operated in the red spectral region. A small portion of this laser beam was taken to servolock the laser to this transition by frequency-modulated Lamb-dip spectroscopy in a neon discharge tube. A second tunable cw single mode dye laser, operated mainly in the blue spectral region, intersected the interaction zone anti-collinearly to the red laser and excited a fraction of the intermediate state population to the $\text{Ne}(ns, nd)$ Rydberg states.

For higher states, especially the $\text{Ne}(nd)$ states, it was important to separate the excitation region from the ion extraction volume (electric field about 4 V/cm), in order to allow for preparation of the Rydberg atoms within an electric field free environment. A simple dual-chamber with graphite-coated walls, as sketched in fig. 1, was found adequate for this pur-

pose and provided clean excitation of $\text{Ne}(ns)$ states up to $n \approx 120$. For $n \lesssim 70$, the Rydberg state population was probed through mass spectrometric detection of the $^{20}\text{Ne}^+$ ions, which were formed – apart from a small background signal – in collisions with thermal energy ($T = 295\text{ K}$) SF_6 molecules in the ion extraction region. For larger n , field ionization in this area became important. For states of lower excitation and shorter lifetime, the excitation volume was shifted towards the ion extraction region to allow the efficient sampling of the product $^{20}\text{Ne}^+$ ions.

The intensity of the red laser was sufficiently attenuated to avoid ac Stark effect, which could be nicely monitored by the ion signal when the blue dye laser was scanned. The typical linewidth (FWHM) was less than 10 MHz and due to the frequency modulation of the red laser ($\approx 4\text{ MHz}$), laser jitter of the blue laser ($\approx 1\text{ MHz}$), residual Doppler effect (about 2 MHz) and transit time effects, when the blue laser was focused (typically 4 MHz).

Wavelength measurements were performed with a travelling Michelson interferometer [11] relative to a polarization-stabilized He-Ne reference laser [12]. Calibration was achieved by comparison with the red dye laser stabilized onto the Lamb-dip of $\text{Ne}(3s-3p)$ lines, which are known to high precision [13]. The reproducibility of our reference wavelength was better than the accuracy of our wavemeter (about 50 MHz). For the experiments discussed in this paper the red laser was always tuned to the favorable $\text{Ne}(3s\ ^3\text{P}_2 \rightarrow 3p\ ^3\text{D}_3)$ transition, for which quenching of the $\text{Ne}(3s\ ^3\text{P}_2)$ flux does not occur [10].

3. Results and discussion

As an example, fig. 2 shows the excitation spectrum of the $\text{Ne}(50d\ J = 2, 3, 4)$ Rydberg states, as detected by collisional ionization with SF_6 . The excitation occurred in the field free region about 1.2 cm upstream from the reaction center. The red excitation laser was strongly attenuated (intensity $< 5\text{ mW/cm}^2$). Higher counting rates may actually be achieved by saturating the first step significantly and tuning the blue laser to one of the components of the Autler-Townes doublet [14]. The SF_6 density was around $2 \times 10^{10}/\text{cm}^3$ for the data in fig. 2. From the spectra of higher Rydberg states it may be inferred that the elec-

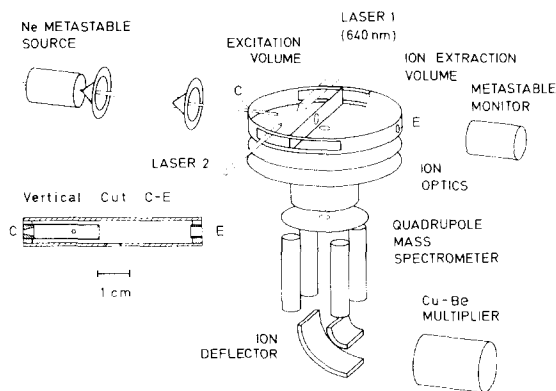


Fig. 1. Semi-schematic view of the experimental setup used for excitation and collisional ionization detection of highly excited neon states. The insert on the left shows a vertical cut of the excitation and reaction double chamber along the axis of the metastable neon beam (C = collimating aperture, E = exit hole). All metal parts of the excitation and reaction chamber are graphite coated to assure uniform surface potentials.

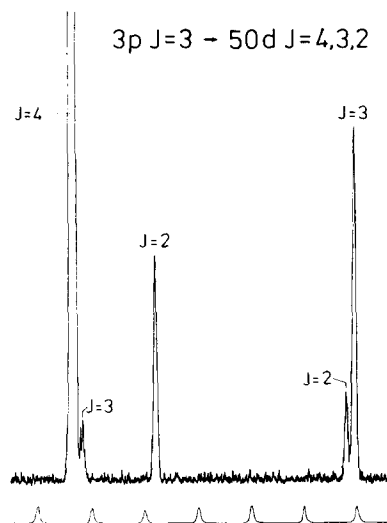


Fig. 2. Laser excitation spectrum of the $\text{Ne}(3p^3D_3 \rightarrow 50d J=2, 3, 4)$ transitions; frequency increases from left to right. The blue dye laser was focused, and the linear polarization of both the red dye laser, exciting the $\text{Ne}(3s^3P_2 \rightarrow 3p^3D_3)$ transition, and the blue dye laser were parallel. The counting rate on the dominant $J=4$ peak, which is about 15 times stronger than the second highest peak ($J=3$), was about 7500/s for the chosen SF_6 -density of about $2 \times 10^{10}/\text{cm}^3$. Frequency markers (lower trace) were taken with a confocal cavity; the free spectral range was measured to be $0.004995(10) \text{ cm}^{-1}$.

tric field in the excitation region was below about 25 mV/cm.

Except for work by Chupka and Hill, quoted in ref. [15] and in ref. [16], respectively, previous studies of collisional ionization of atomic Rydberg states with SF_6 did not extend significantly to n -values below 20. We have observed effective ionization of Ne Rydberg states with binding energies up to 0.38 eV ($\text{Ne}(6d)$). Unfortunately, our laser system so far did not allow a study with $\text{Ne}(6s, 7s)$ and $\text{Ne}(5d)$, for which electron transfer to SF_6 may be expected [16] to occur, too. For $\text{Ne}(5s J=2)$ and $\text{Ne}(4d J=4)$, we could not detect a relevant signal due to collisional ionization with SF_6 ; these states were, however, easily converted to ions by photoionization with either laser (depending on the relative intensities of the two lasers). We note that photoionization was a small to undetectable effect for the higher studied states under our experimental conditions.

From measurements with different target densities and several distances between excitation region and ion extraction volume we have estimated the absolute cross section q for collisional ionization of several $\text{Ne}(ns, nd)$ states to within a factor of 2. These cross sections are weakly n -dependent and in the range $(3 \pm 2) \times 10^{-12} \text{ cm}^2$ for $n \geq 10$, but decrease substantially with rising electron binding energy for the lower n .

Comparison with other work [5,6,17,18] should be made on the basis of the experimental rate constants k , related with q through $k = qv_{\text{rel}}$ (v_{rel} = relative velocity of the colliding heavy particles). In this way, the expected $(1/v_{\text{rel}})$ -dependence of q is accounted for, which was demonstrated experimentally by Dimicoli and Botter [17] and just reflects the total amount of time available for the collision system to pass the effective reaction zone; one should observe the same k for collision systems with identical v_{rel} and n . Unfortunately, the agreement between the different available data [5,6,17,18] for $k(\text{SF}_6)$ in the common range of $n \approx 20$ –30 is rather poor; it is not clear to which degree this may be attributed to different l -distributions, associated with the primary and secondary (e.g. blackbody radiation induced [19]) excitations. What is important in the context of Rydberg detection, however, is the fact that the rate constant for collisional ionization is very large for $n \geq 10$ with values around $2 \times 10^{-7} \text{ cm}^3/\text{s}$. For $\text{Ne}(6d) + \text{SF}_6$, the rate constant is about two orders of magnitude smaller, but still sufficiently large to allow the production of substantial ion signals.

Although in the present work the negative product ions have not been detected, it is clear from the earlier work [6,16,17] and from energy conservation that the collisionally produced $^{20}\text{Ne}^+$ ions are created along with SF_6^- ions. Allowing for 60 meV average relative collision energy, the observation of the ion pair formation process with $\text{Ne}(6d)$ atoms suggests that the electron affinity of SF_6 is at least 0.32 eV, in agreement with previous work [20,21]. As long as nothing is known about the relative kinetic energy of the product ions and about the internal final state distribution of SF_6^- , any conclusion on the electron affinity of SF_6 from the observation or non-observation of process (2) is uncertain, however. Therefore, the non-observation of Ne^+ for reactions of $\text{Ne}(5s)$ and $\text{Ne}(4d)$ (binding energies of 1.00 eV and 0.86 eV, resp.) does not

exclude that $EA(SF_6)$ may be as large as 1 eV, a value recently proposed by Streit [21].

As for the mechanism of process (2), it is generally believed that for high n ($\gtrsim 20$) the process is analogous to electron attachment of a quasi-free electron, with the core of the Rydberg atom playing the role of a spectator. Work by Klots [22] and by Astruc et al. [23] on the autodetachment and dissociation processes of the SF_6^- ion, formed in collisions with Ar^{**} and He^{**} atoms (produced by electron impact excitation), indicated, however, that (partial) stabilization of the SF_6^- occurs by collisions with the Rydberg core. How stabilizing $A^+ + M^-$ encounters come about in the course of process (2), can be easily seen within the following simple reaction model: let us assume that the range b_c of contributing impact parameters is given by the de Broglie wavelength of the transferred electron $\lambda_n \approx n^2 a_0$ (a_0 = Bohr radius). We visualize that electron transfer happens suddenly at some large internuclear distance $R \lesssim b_c$, i.e. the distance between the nuclei remains practically unchanged during electron transfer and the collision system now consists of two rather compact Coulomb centers with potential energy $-e^2/(4\pi\epsilon_0 R)$. The kinetic energy of the heavy particles does not change during electron transfer and is approximately equal to the asymptotic relative collision energy E_{rel} . If $R < R_d = e^2/(4\pi\epsilon_0 E_{rel})$ ($R_d = 450 a_0$ for our $E_{rel} = 60$ meV) the intermediate ionic complex will not be able to directly separate into the dissociated products A^+ and M^- . As a result, scattering of A^+ from M^- accompanied by energy exchange will be possible. Transfer of internal, e.g. vibrational, energy of M^- into relative kinetic energy of the $A^+ - M^-$ system will enable subsequent dissociation of the ionic complex. The final state M^- ion has less internal energy than the one created upon electron attachment in the primary step, and this corresponds to "stabilization" of M^- [22, 23]. For lower n -states ($n \lesssim 21$ for $E_{rel} = 60$ meV) electron transfer happens for distances $R < R_d$; therefore, within the described model, stabilizing encounters between A^+ and M^- are necessary for product formation (i.e. dissociation) for lower n .

For very low n , i.e. when λ_n is not distinctly larger than the sum of the diameters of A^+ and M^- , a description of process (2) as a two step process is no longer realistic; in particular, the quasi-free electron aspect of the primary step is no longer fulfilled. For a detail-

ed test of the mechanism for process (2), it would be very valuable to determine the kinetic energy and angular distribution of the ionic products in the range from very low to high n , where the quasi-free electron model is expected to be correct.

The application of the SF_6 collisional ionization detection technique for spectroscopic studies of Rydberg states with effective quantum numbers $n^* \gtrsim 6$ is straightforward in all those cases where collimated beams of atoms or molecules are available for excita-

Table 1

Measured transition energies [cm^{-1}] for the $^{20}Ne(3p J = 3 \rightarrow nd J = 4)$ series. The individual uncertainties are $\pm(2-3) \times 10^{-3} cm^{-1}$. The energy for the $^{20}Ne(3s J = 2 \rightarrow 3p J = 3)$ transition was determined as $15\,615.1963(20) cm^{-1}$

n	Transition energy	n	Transition energy
4	17 342.9913	39	24 200.5030
6	21 201.4270	40	24 204.0664
7	22 018.4312	41	24 207.3811
8	22 548.0897	42	24 210.4570
9	22 910.8825	43	24 213.3232
10	23 170.1802	44	24 215.9953
11	23 361.9076	45	24 218.4879
12	23 507.6547	46	24 210.8229
13	23 621.0253	47	24 223.0084
14	23 710.9461	48	24 225.0614
15	23 783.4658	49	24 226.9869
16	23 842.7973	50	24 228.7993
17	23 891.9593	51	24 230.5062
18	23 933.1433	52	24 232.1175
19	23 967.9936	53	24 233.6355
20	23 997.7408	54	24 235.0708
21	24 023.3341	55	24 236.4278
22	24 045.5146	56	24 237.7121
23	24 064.8639	57	24 238.9329
24	24 081.8418	58	24 240.0904
25	24 096.8213	59	24 241.1866
26	24 110.1070	60	24 242.2283
27	24 121.9408	61	24 243.2206
28	24 132.6279	62	24 244.1654
29	24 142.0388	63	24 245.0652
30	24 150.6137	64	24 245.9252
31	24 158.3730	65	24 246.7431
32	24 165.4129	66	24 247.5262
33	24 171.8242	67	24 248.2714
34	24 177.6776	68	24 248.9883
35	24 183.0343	69	24 249.6698
36	24 187.9423	70	24 250.3247
37	24 192.4751	71	24 250.9533
38	24 196.6456	72	24 251.5530

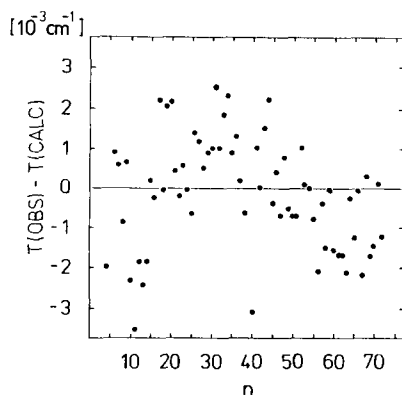


Fig. 3. Differences between observed and calculated (see text) term values for the measured $^{20}\text{Ne}(nd\ J=4)$ energy levels.

tion under conditions such as those sketched in fig. 1. The method is convenient and sufficiently sensitive to allow spectroscopy with beams of considerably lower flux than the ones used here. It works equally well with cw and pulsed excitation. We think that it presents an attractive alternative to combined field ionization/fluorescence detection and to the use of thermionic diodes [24].

We have used the SF_6 collisional ionization scheme for detection of a large number of $^{20}\text{Ne}(ns, nd)$ Rydberg states in connection with a careful spectroscopic study to be described in detail elsewhere. Other recent spectroscopic work on highly excited $\text{Ne}(ns, nd)$ states [26,27] was limited in accuracy by its comparatively large frequency bandwidth of about 50 GHz. We have found that the $\text{Ne}(nd\ J=4)$ series ($n=4, 6-72$) is unperturbed and can be very well described by the one-channel formula [25]:

$$T(n^*) = \text{IP} - R/n^{*2}, \quad (3)$$

with $n^* = n - c_0 - c_2/n^{*2}$.

Experimentally, the energy difference $T(n^*) - T(3s\ ^3P_2)$ is measured as the sum of the energies for the $^{20}\text{Ne}(3s\ J=2 \rightarrow 3p\ J=3)$ and $^{20}\text{Ne}(3p\ J=3 \rightarrow nd\ J=4)$ transitions (see table 1). The ionization potential $\text{IP}(^2P_{3/2})$, which is included as a fit parameter, is determined accurately *relative* to $T(3s\ ^3P_2)$. From a least squares fit to the 68 data points, we obtain: $c_0 = 0.02423(2)$, $c_2 = -0.05674(9)$, and $\text{IP}(^2P_{3/2}) - T(3s\ ^3P_2) = 39\,887.9326(6)\text{ cm}^{-1}$ (4)

Fig. 3 shows the corresponding energy differences between the measured data points and positions calculated with the given parameters c_0 , c_2 , and the difference (4).

$T(3s\ ^3P_2)$ so far is only known to within $\pm 0.04\text{ cm}^{-1}$ [28]. Its value for natural neon is $T(3s\ ^3P_2)_{\text{Ne}}^{\text{nat}} = 134\,041.840(40)\text{ cm}^{-1}$ [28]. The value for ^{20}Ne is expected to be 0.03 cm^{-1} smaller [28]. Therefore, we have

$$\text{IP}[^{20}\text{Ne}+(^2P_{3/2})] = 173\,929.743(40)\text{ cm}^{-1}, \quad (5)$$

in agreement with the less precise values given by Kaufman and Minnhagen [28] and by Baig and Connerade [27].

Acknowledgement

This work was supported by the Deutsche Forschungsgemeinschaft (Sonderforschungsbereich 91) and by the Bundesministerium für Forschung und Technologie. We thank H. Rinneberg for the loan of the Fabry-Perot marker cavity.

References

- [1] Rydberg states of atoms and molecules, eds. R.F. Stebbings and F.B. Dunning (Cambridge University Press, 1983).
- [2] D. Kleppner, M.G. Littman and M.L. Zimmermann, review in ref. [1], p. 73 f.
- [3] V. Cermak and Z. Herman, Coll. Czech. Chem. Commun. 29 (1964) 953.
- [4] F. Gounand and J. Berlande, review in ref. [1], p. 229 f.
- [5] F.B. Dunning and R.F. Stebbings, review in ref. [1], p. 315 f.
- [6] H. Hotop and A. Niehaus, J. Chem. Phys. 47 (1967) 2506.
- [7] H. Hotop and A. Niehaus, Z. Physik 215 (1968) 395; H. Hotop, Diplomarbeit, Universität Freiburg, 1967 (unpubl.).
- [8] L.G. Christophorou, Adv. Electron. Electron Phys. 46 (1978) 55; A. Chutjian, Phys. Rev. Lett. 46 (1981) 1511.
- [9] E. Fermi, Nuovo Cimento 11 (1934) 157; M. Matsuzawa, review in ref. [1], p. 267 f.
- [10] A. Siegel, J. Ganz, W. Bussert and H. Hotop, J. Phys. B: At. Mol. Phys. 16 (1983) 2945.
- [11] J.L. Hall and S.A. Lee, Appl. Phys. Lett. 29 (1976) 367.
- [12] S.J. Bennett, R.G. Ward and D.C. Wilson, Appl. Optics 12 (1973) 1406.

- [13] S.R. Amin, J. Opt. Soc. Am. 73 (1983) 862;
J.C. Bergquist and H.U. Daniel, Optics Comm. 48 (1984) 327.
- [14] S.H. Autler and C.H. Townes, Phys. Rev. 100 (1955) 703;
P.L. Knight and P.W. Milonni, Phys. Rep. 66 (1980) 21.
- [15] D. Kleppner, Atomic Physics, 5, eds. R. Marcus, M. Prior and H. Shugart (Plenum Press, 1977) p. 269 f, fig. 1.
- [16] R.M. Hill, work cited in ref. [5], pages 338–340.
- [17] I. Dimoclo and R. Botter, J. Chem. Phys. 74 (1981) 2346, 2355.
- [18] B.G. Zollars, K.A. Smith, and F.B. Dunning, J. Chem. Phys. 81 (1984) 3158.
- [19] T.F. Gallagher, review in ref. [1], p. 165 f.
- [20] P.S. Drzaic, J. Marks and J.I. Brauman, in: Gas phase ion chemistry, ed. M.T. Bowers, Vol. 3 (Academic Press, New York, 1984) p. 167 f.
- [21] G.E. Streit, J. Chem. Phys. 77 (1982) 826.
- [22] C.E. Kolts, J. Chem. Phys. 66 (1977) 5240.
- [23] J.P. Astruc, R. Barbé and J.P. Schermann, J. Phys. B: At. Mol. Phys. 12 (1979) L377;
J.P. Astruc, R. Barbé, A. Lagréze and J.P. Schermann, Chem. Phys. 75 (1983) 405.
- [24] K. Niemax, in: The physics of ionized gases, ed. G. Pichler (IFIS, Zagreb, 1983) p. 333 f.
- [25] M.J. Seaton, Proc. Phys. Soc. 88 (1966) 815.
- [26] T. Caesar and J.-L. Heully, J. de Physique 44 (1983) C7-261.
- [27] M.A. Baig and J.P. Connerade, J. Phys. B: At. Mol. Phys. 17 (1984) 1785.
- [28] V. Kaufman and L. Minnhagen, J. Opt. Soc. Am. 62 (1972) 92.